Observed twin gyres and their interannual variability in the equatorial Indian Ocean using Topex/Poseidon altimetry

B. H. Vaid*, C. Gnanaseelan and P. S. Salvekar

Indian Institute of Tropical Meteorology, Dr Homi Bhabha Road, Pune 411 008, India

Recent numerical models have simulated the equatorial Indian Ocean twin gyres. However, there is no strong observational evidence for the existence of these gyres. Satellite technology and filter techniques are explored in this study to provide observational evidence for the existence of these gyres. The westward-propagating Rossby waves in the equatorial Indian Ocean, filtered from the Topex/Poseidon sea surface height anomalies (SSHA) showed the twin gyre structure which coincides with the model-simulated gyres. The present study further addresses the interannual variability of these gyres, especially during the Indian Ocean Dipole (IOD) years. The anomalous wind stress curl is found to drag the annual Rossby waves during the IOD years in the region 78°E–88°E. The downwelling favourable wind stress curl deepens the thermocline and increases SSHA and sea surface temperature.

Keywords: Indian Ocean Dipole, interannual variability, Rossby waves, twin gyres.

WESTWARD-propagating twin gyres in the equatorial Indian Ocean were first reported by Reddy *et al.*[1] using their model simulated currents. They could not find the twin gyres in the raw Topex/Poseidon (T/P) sea surface height anomalies (SSHA), and suggested that SSH variations do not precisely capture the twin-gyre structure. Moreover, it is difficult and expensive to design a programme to observe these currents. Thus it was felt that the T/P SSHA, which is the best remote-sensing source available to observe SSHA (unprecedented accuracy of 2 cm) could be used to explore the existence of these gyres. The formation of twin gyres is due to the nonlinear interaction between the equatorial jet and the first-mode Rossby waves at the front of the reflected packet. In this study the SSHA data are filtered using finite impulse response (FIR) filter to extract these gyres. Thus the present study reports the twin gyres structure from the T/P SSHA.

Reddy *et al.*[1] emphasized that the twin gyres develop every year during 1992–2001 with less interannual variability. They did not pay attention to the variability during the Indian Ocean Dipole (IOD) years. The IOD is a climate mode that occurs in the tropical parts of the Indian Ocean. Usually, the sea surface temperature (SST) is low in the western Indian Ocean and high in the eastern Indian Ocean. However, during some years this SST gradient reverses and causes a shift of convective activities over the western equatorial Indian Ocean. This has been identified as IOD or zonal anomaly of the SST in the equatorial Indian Ocean[2,3]. The present study investigates the interannual variability in the Rossby waves in the equatorial Indian Ocean during the IOD years 1994 and 1997–98. This is an extension of the study by Reddy *et al.*[1] mainly in the following aspects: (a) providing observational support to twin-gyre structure from the T/P SSHA and (b) understanding interannual variability in the westward-propagating twin gyres in the equatorial Indian Ocean during the IOD years.

*For correspondence. (e-mail: bhv@tropmet.res.in)

Data and methodology

This study used the T/P data distributed by the Jet Propulsion Laboratory Physical Oceanography Distributed Active Archive Center (JPL/PODAAC) published for the World Ocean Circulation Experiment Conference (WOCE global data, version 1.1, 1998). The data consist of SSHA in relation to a 5-yr average (1993–98) and are presented in bin-averaged grid maps of $0.5° \times 0.5° \times 10$ days. The data cover latitudes between 66°S and 66°N, and from October 1992 to December 2002. All the standard corrections have been applied[4]. η_o is bicubically interpolated to a $1° \times 1°$ grid. Maps of original $\eta_o(x,t)$, T/P SSHA are converted to diagrams of, $\eta_o(x,t)$ one for every degree of latitude. Data over shallow areas (depth $H \leq -1000$ m), small islands ($x \leq 3°$) and zonally enclosed water bodies have been excluded to facilitate filtering. Only continuous open-ocean areas with zonal dimension in excess of 20°, wide enough to apply the filter, were used. Each η_o data matrix was decomposed through a 2D zonal–temporal filter.

FIR filters are based on convolution of two sequences, the original data η_o, and the filter f, resulting in the filtered data η_f. The statistical significance of these signals is measured by the amplitude A, fractional variance V, and the signal-to-noise ratio S/N estimated for each component. If no statistically significant wave signal is present

for a given spectral band, the filtered signal will have very low amplitude, explain little or nothing of the total variance, and have a *S/N* ratio of nearly zero. In the present case, $\eta_o(x,t)$ is a function of longitude and time. Therefore, the filter $f(i,j)$ is a function of longitudinal lag i and temporal lag j. The filtered matrix $\eta_f(x,t)$ is obtained from:

$$\eta_f(x,t) = \sum_{i=-m}^{m} \sum_{j=-n}^{n} \eta_o(x+i, t+j) f(i,j). \quad (1)$$

For the band-pass filtering of the annual and semi-annual Rossby wave components (say η_{12}, η_6), the filter $f(i,j)$ is a Gaussian tapered cosinusoidal surface:

$$f(i,j) = \frac{e^{-1/2((\pi i/m)^2 + (\pi j/n)^2)}}{N} \cos\left(\frac{2\pi i}{L} - \frac{2\pi j}{T}\right) + M, \quad (2)$$

$$\text{with } M \text{ and } N \text{ such that } \begin{cases} \sum_{i=-m}^{m} \sum_{j=-n}^{n} |f(i,j)| = 1, \\ \sum_{i=-m}^{m} \sum_{j=-n}^{n} f(i,j) = 0, \end{cases}$$

where L and T are the wavelength and period of the approximate centre of each band. T was set to 365 and 183 days and L was such that $L = CpT$. The filter size parameters m and n were set to one period and one wavelength. The Gaussian part of eq. (2) works as a smoother, while the cosine part limits the power of the response to a specific area in the 2D spectrum. This can be understood as a 2D version of the tapered cosine window functions (Blackman, Hamming, Hanning, etc.) used in classical 1D spectral analysis, whose main advantages are the same: to minimize phase distortion and to reduce the amplitude of side-lobes (leaking). More detailed description of the filtering technique and its performance is available in the literature[5–9]. The filter used in this study is not a function of latitude. It is a function of only longitude and time, but is applied to all the latitudes.

The need for FIR filters arises from the difficulty inherent in the measurement of phase propagation of waves with a broad spectrum. FIR filters work through convolution in the space–time domain, in a way that is conceptually similar to wavelets. Both methods work well with signals whose spectral power distribution changes with time because they act locally, unlike methods based on Fourier transform that processes the whole series at once. In both wavelets and FIR filters the convolutions are applied first over the larger wavelengths and longer periods, and then over smaller wavelengths and shorter periods. This strategy gives better results because when the smaller scales are processed, the field is already locally detrended by the previous removal of larger scales. By better results we mean that the spectral 'band' of the filtered signal is narrower.

The FIR filter method offers an alternative, where each filter component covers a finite range of periods and wavelengths, a spectral band instead of a spectral line. Amplitudes, periods and wavelengths can vary within certain thresholds, with the period chosen a priori, centred within the bandwidth. No functional shape is assumed and the data are processed simultaneously in the time and longitude domains. This makes the filter design process more intuitive and thus easier to adapt to oceanographic applications in which two out of the three parameters Cp, T and L, are known to be within a certain range. The filter parameters are adjusted to bracket the spectral bands related to previously observed physical processes (e.g. seasonality, Rossby and Kelvin waves). This is an advantage to classical Fourier analysis and complex empirical orthogonal functions, since both methods do not allow for such adjustment. A complete description of FIR filters used in this study is given in Vaid *et al.*[10].

Results and discussion

Twin gyre structure in the TP SSHA and its interannual variability

The westward-propagating Rossby waves have a broad spectrum dominated by semi-annual and annual signals, whose amplitudes vary significantly with time. The equatorial jet (or Wyrtki jet) has been thoroughly examined in previous studies. However, how reflected Rossby waves from the Sumatra coast interact with the incident equatorial jet has not been investigated in detail yet. The propagation of equatorial Rossby waves is seen as twin gyres, with one gyre centred in the northern hemisphere and the other in the southern hemisphere. Propagation of the equatorial semi-annual Rossby waves during 1994 and 1997 (positive IOD years) is shown in Figure 1. During 1994 and 1997, the twin gyres formed by the end of May, one just north of the equator and the other south of it. The northern gyre in 1994 was centred along 4.5°N and the weaker southern gyre along 5.5°S. In contrast, in 1997 the northern gyre was centred along 3.5°N and its southern counterpart along 4.5°S. These semi-annual Rossby waves (or twin gyres) were observed to reach the western Indian Ocean during August/September. Figure 2 shows the semi-annual Rossby waves during the years following the above IOD years. During this time, the gyres reached the western Indian Ocean in October/November. The reverse Wyrtki jet during the dipole years[11,12] led to faster propagation of semi-annual Rossby waves during the IOD years. Recent studies have shown the reversed/weak Wyrtki jets during the IOD years. During 1995, the northern gyre was seen propagating with its centre along 4.5°N. The southern gyre was centred along 4.5°S throughout 1995. In 1998,

the northern gyre was found along 2.5°N and southern gyre along 4.5°S, but the northern gyre had strengthened near 60°E.

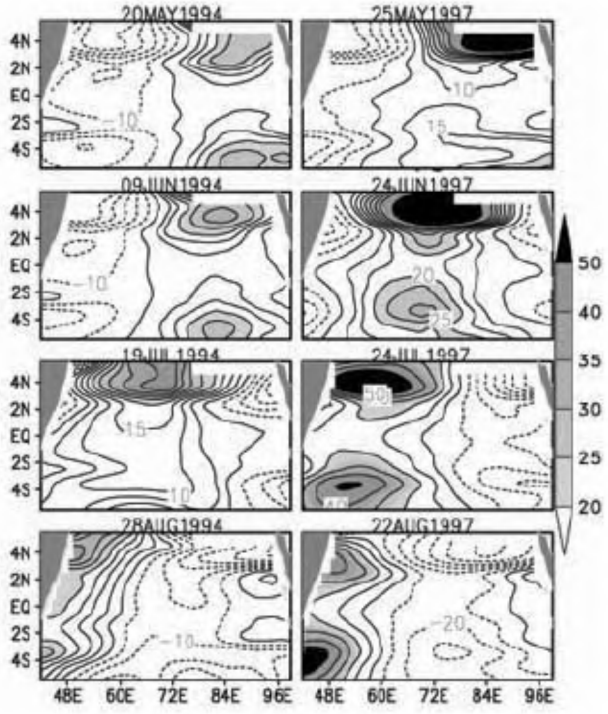

Figure 1. Propagation of semi-annual Rossby waves (mm) during 1994 and 1997.

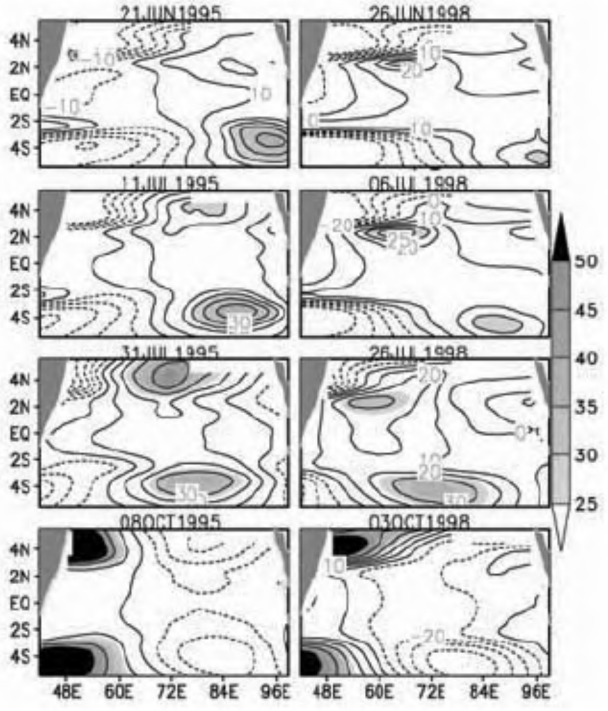

Figure 2. Propagation of semi-annual Rossby waves (mm) during 1995 and 1998.

The propagation of annual Rossby waves during the positive dipole years of 1994 and 1997 is shown in Figure 3. The southern gyres in 1994 and 1997 were dominant and centred along 6.5°S and the weaker northern gyres were centred along 2.5°N. The intense southern gyre is associated with the IOD forcing which mostly originated in the southeastern equatorial Indian Ocean. During 1997, the strong westward propagating annual Rossby waves were observed in the eastern boundary around June, and they reached the western boundary in February/March 1998. Whereas the semi-annual signals reached the western boundary in October/November 1997. The annual signals of 1994 reached the western boundary in February/March 1995. In contrast, Figure 4 shows annual Rossby waves in 1995 and 1998, with the northern gyre centred along 2.5°N and the southern gyre along 3.5°S. The Rossby wave propagation as twin gyres was observed not only in the IOD years, but also during the study period, with considerable interannual variability in both intensity and latitudinal extent. These Rossby waves have a local minimum along the equator with symmetric maxima between 4.5°N and 4.5°S, in agreement with earlier studies[13,14]. But during the IOD years Rossby waves are found to have a pattern different from the normal years. The phase speeds of semi-annual and annual Rossby waves were estimated using radon transform method[6]. For semi-annual Rossby waves the phase speed along 2.5°N was –41 cm/s, 4.5°N is –49 cm/s and 4.5°S is –63 cm/s. For annual Rossby waves along 2.5°N, 3.5°S and 6.5°S, the phase speeds were observed to be –33, –35 and –24 cm/s respectively.

Identification of Rossby waves as equatorial twin gyres in the SSHA will add a new insight into the Indian Ocean dynamics. One possibility for the genesis of the twin gyres is the nonlinear interaction between the equatorial jet and the first-mode Rossby waves in front of the reflected packet[1]. According to this view, it is the strong retarding effect of the equatorial jet that allows a soliton-like twin-gyre structure to develop at the wave front. Another possibility is that the gyres are Rossby wave solitons[15], and the soliton theory involves only the Rossby waves balancing nonlinearity against depression. The oceanic wave propagation can also cause local wind stress anomalies to remotely influence the thermocline depth and the SST[16].

Drag or slowing down of westward propagating twin gyres

The gyres that formed in 1994 and 1997 reached the western boundary in February/March 1995 and 1998 respectively (Figure 3). In contrast, gyres that formed in 1995 and 1998, the years following IOD (Figure 4), propagated relatively faster and reached the western boundary in October/November of the same year. We examined the propagation of annual Rossby waves in the

rest of the non-IOD years during the study period and found faster propagation similar to those obtained in 1995 and 1998 (figure not shown). From the detailed analysis of the annual Rossby wave signals during the IOD years, a drag in the propagation of annual Rossby waves was observed in the region 78°E–88°E (Figure 5). The average annual Rossby wave phase speed during the dipole years was approximately –29 cm/s along 3.5°S, whereas in the other years it was approximately –37 cm/s.

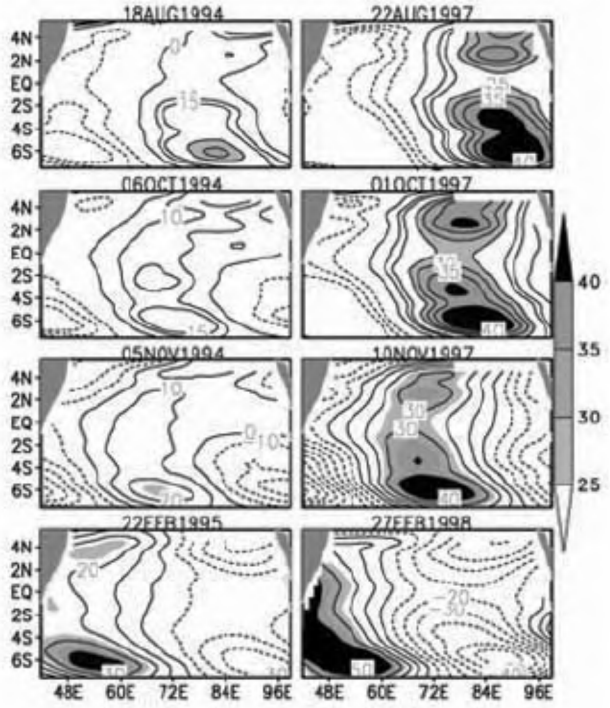

Figure 3. Propagation of annual Rossby waves (mm) during 1994 and 1997.

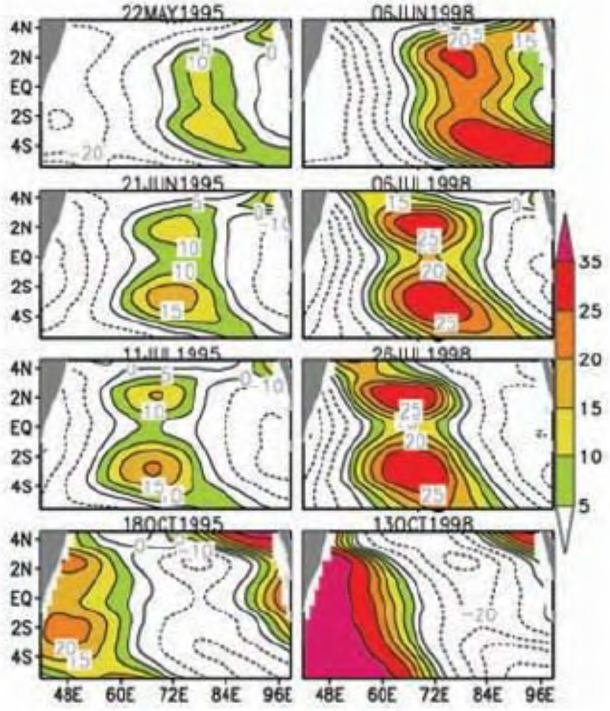

Figure 4. Propagation of annual Rossby waves (mm) during 1995 and 1998.

Rossby wave characteristics (amplitude and propagation speed) can be altered by wind or buoyancy forcing that is phase-locked with the wave signal[17]. Figure 6 *a* shows area-averaged wind stress curl anomaly over 78°E–88°E, 6.5°S–4.5°N (Box 1) and Figure 6 *b* shows zonal wind stress anomaly, meridional wind stress anomaly, and wind stress anomaly averaged over Box 1. The anomalous wind stress and wind stress curl during the dipole years drag the annual Rossby waves in the region 78°E–88°E. Variation of wind stress and wind stress curl deepens the thermocline and reduces the phase speed of the Rossby waves. Wind stress over the Indian Ocean was computed from NCEP/NCAR winds and anomalies of all the parameters considered in the study were computed by removing corresponding monthly climatologies.

Impact of slowing down of twin gyres on equatorial Indian Ocean

Figure 7 *a* shows optimum interpolated SST version 2 anomalies (IOSSTA) over Box 1 and Box 2 (88°E–98°E, 6.5°S–4.5°N). Figure 7 *b–d* shows T/P SSHA kinetic energy and heat storage over Box 1 and Box 2 respectively. The difference in these values in the boxes is usually negligible during the normal years, whereas considerable difference is observed in the dipole years. Heat storage anomalies are derived from $\Delta H = \rho C p \Delta(\eta)/\alpha$, where ρ is

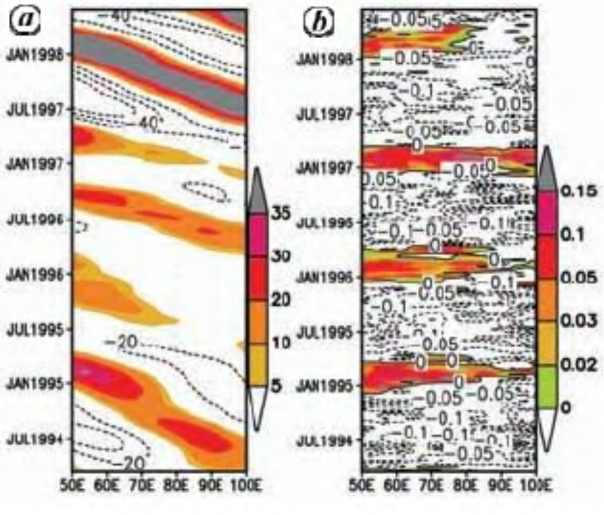

Figure 5. Time–longitude plot averaged over 6.5°S to 3.5°S. ***a***, Annual Rossby wave. ***b***, Wind stress curl.

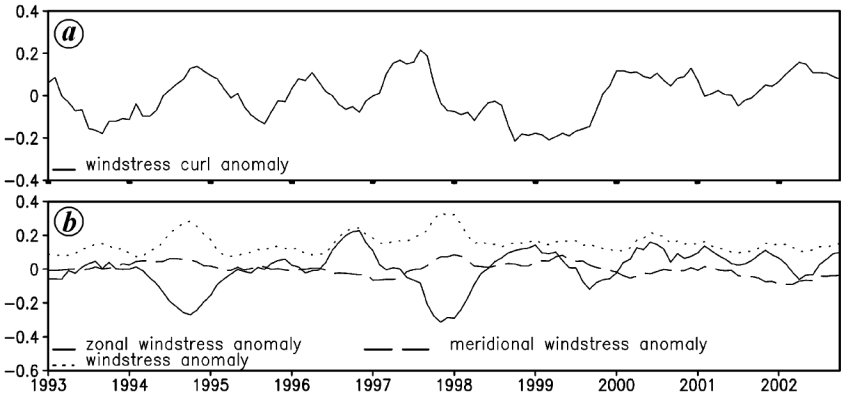

Figure 6. ***a***, Wind stress curl anomaly (*10^8 dyn/cm^3) averaged over 78°E–88°E, 6.5°S–4.5°N (solid line). ***b***, Zonal wind stress anomaly (dyn/cm^2), meridional wind stress anomaly (dyn/cm^2) and wind stress anomaly (dyn/cm^2) averaged over 78°E–88°E, 6.5°S–4.5°N.

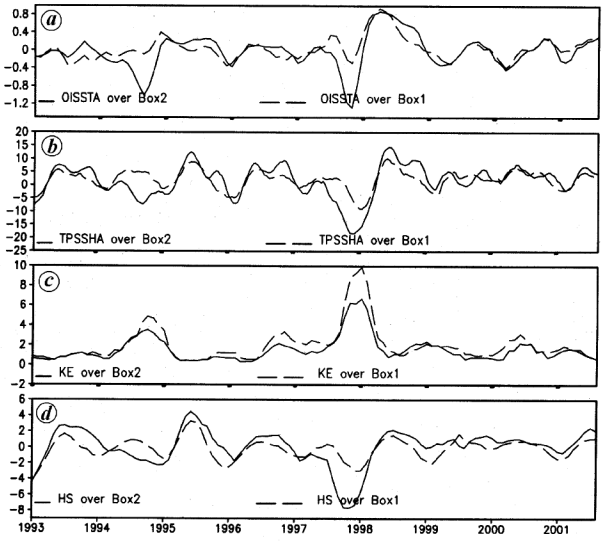

Figure 7. ***a***, Optimum interpolated SSTA (OISSTA) over Box 1 (78°E–88°E, 6.5°S–4.5°N) and Box 2 (88°E–98°E, 6.5°S–4.5°N). ***b–d***, TPSSHA (***b***), kinetic energy (kg m^2/s^2) (***c***) and heat storage (10^8 J/m^2) (***d***) over Box 1 and Box 2.

the water density (1027 kg/m^3), Cp is the specific heat at constant pressure and α is the thermal expansion coefficient values (same as those used by Chambers and Tapley[18]). Thermal expansion coefficient values (α) used in heat storage computation are the climatological values based on Chambers and Tapley[18] and are same for IOD years and normal years. It is speculated that the drag (or slow down) in the Rossby waves during the dipole years in the region 78°E–88°E might give more energy (4 kg m^2/s^2). The increase in SSHA (10 cm) and SSTA (1°C) observed in Box 1 is associated with the downwelling favourable wind stress curl anomalies (Figures 6 and 7).

Summary

T/P SSHA from JPL/PODAAC have been used to study the annual and semi-annual Rossby wave propagation in the tropical Indian Ocean. The propagation of equatorial annual and semi-annual Rossby waves was observed as twin gyres with minima along equator and maxima on either side of the equator. This study provides observational evidence for the existence of twin gyres in the tropical Indian Ocean using T/P SSHA. The formation of twin gyres is due to the nonlinear interaction between the equatorial jet and the first-mode Rossby waves at the front of the reflected packet. During the IOD years of 1994/1995 and 1997/1998, the annual Rossby waves propagate slower (than normal) and reach the western boundary three to four months later. The average annual Rossby wave phase speed during the dipole years was approximately –29 cm/s along 3.5°S, whereas in other years it was approximately –37 cm/s. A drag in the propagation of annual Rossby waves was observed in the region 78°E–88°E during the IOD years which affect the SSHA and SSTA over the region (78°E–88°E). The anomalous wind stress and wind stress curl seem to play an important role in dragging the propagation of annual Rossby waves in the region 78°E–88°E. Hence the annual Rossby waves arrive in the western Indian Ocean late in February/March during the IOD years.

1. Reddy, P. R. C., Salvekar, P. S., Deo, A. A. and Ganer, D. W., Westward propagating twin gyres in the equatorial Indian Ocean. *Geophys. Res. Lett.*, 2004, **31**, L01304.
2. Saji, N. H., Goswami, B. N., Vinayachandran, P. N. and Yamagata, T., A dipole mode in the tropical Indian Ocean. *Nature*, 1999, **401**, 360–363.
3. Webster, P. J., Moore, A. M., Loschnigg, J. P. and Leben, R. R., Coupled ocean–atmosphere dynamics in the Indian Ocean during 1997–98. *Nature*, 1999, **401**, 357–360.

4. Benada, R. J., Merged GDR (TOPEX/POSEIDON), Generation B Users Handbook, Version 2.0; Physical Oceanography Distributed Active Archive Center (PODAAC), Jet Propulsion Laboratory, Pasadena, 1997, JPL, D-11007.
5. Polito, P. S. and Cornillon, P., Long barocilinic Rossby waves detected by Topex/Poseidon. *J. Geophys. Res.*, 1997, **102**, 3215–3235.
6. Polito, P. S., Sato, O. T. and Liu, W. T., Characterization and validation of the heat storage variability from TOPEX/POSEIDON at four oceanographic sites. *J. Geophys. Res.*, 2000, **105**, 16911–16921.
7. Polito, P. S. and Liu, W. T., Global characterization of Rossby waves at several spectral bands. *J. Geophys. Res.*, 2003, **108**, 3018.
8. Gnanaseelan, C., Vaid, B. H., Polito, P. S. and Salvekar, P. S., Interannual variability of Kelvin and Rossby waves in the Indian Ocean from Topex/Poseidon altimetry data. IITM Research Report, 2004, RR-103, 35.
9. Gnanaseelan, C., Vaid, B. H. and Polito, P. S., Impact of biannual Rossby waves on Indian Ocean Dipole. *IEEE Geosci. Remote Sensing Lett.*, 2008, **5**, 427–429.
10. Vaid, B. H., Gnanaseelan, C., Polito, P. S. and Salvekar, P. S., Influence of Pacific on southern Indian Ocean Rossby waves. *Pure Appl. Geophys.*, 2007, **164**, 1765–1785.
11. Thompson, B., Gnanaseelan, C. and Salvekar, P. S., Variability in the Indian Ocean circulation and salinity and their impact on SST anomalies during dipole events. *J. Mar. Res.*, 2006, **64**, 853–880.
12. Sharma, R., Agarwal, N., Basu, S. and Agarwal, V. K., Impact of satellite-derived forcings on numerical ocean model simulations and study of sea surface salinity variations in the Indian Ocean. *J. Clim.*, 2007, **20**, 871–890.
13. Delcroix, T., Picaut, J. and Eldin, G., Equatorial Kelvin and Rossby waves evidenced in the Pacific Ocean through Geosat sea level and surface current anomalies. *J. Geophys. Res.*, 1991, **96**, 3249–3262.
14. Chelton, D. B. and Schlax, M. G., Global observations of Rossby waves. *Science*, 1996, **272**, 234–238.
15. Boyd, J. P., Equatorial solitary waves, Part 1: Rossby solitons. *J. Phys. Oceanogr.*, 1980, **10**, 1699–1717.
16. Holton, J., *An Introduction to Dynamic Meteorology*, Academic Press, Amsterdam, 2004, 4th edn.
17. White, W. B., Annual forcing of baroclinic long waves in the tropical North Pacific. *J. Phys. Oceanogr.*, 1977, **7**, 50–61.
18. Chambers, D. P. and Tapley, B. D., Long-period ocean heat storage rates and basin scale heat fluxes from Topex. *J. Geophys. Res.*, 1997, **102**, 10525–10533.

ACKNOWLEDGEMENTS. We thank the Director, IITM, Pune and Head, TSD, IITM for support. We also thank Dr P. S. Polito for FIR filter and Dr J. P. McCreary for support, encouragement and suggestions. The financial support was provided by INCOIS Hyderabad. Dr D. P. Chambers provided thermal expansion coefficients for calculating heat storage. Comments from the two anonymous reviewers helped improve the manuscript.

Received 17 October 2007; revised accepted 8 May 2008